SIAM J. SCI. COMPUT.
Vol. 19, No. 2, pp. 319–340, March 1998

SOLUTION OF TWO-DIMENSIONAL RIEMANN PROBLEMS OF GAS DYNAMICS BY POSITIVE SCHEMES*

PETER D. LAX† AND XU-DONG LIU†

Abstract. The positivity principle and positive schemes to solve multidimensional hyperbolic systems of conservation laws have been introduced in [X.-D. Liu and P. D. Lax, *J. Fluid Dynam.*, 5 (1996), pp. 133–156. Some numerical experiments presented there show how well the method works. In this paper we use positive schemes to solve Riemann problems for two-dimensional gas dynamics.

Key words. positive scheme, two-dimensional Riemann problem, shock

AMS subject classifications. 35, 65, 76

PII. S1064827595291819

1. Introduction.

Over the last decade a great deal of effort has been devoted to designing total variation diminishing (TVD) numerical schemes for solving hyperbolic conservation laws; see Harten's basic paper [5]. Strictly speaking, TVD schemes exist only for scalar conservation laws and for linear hyperbolic systems in one space variable. However, hyperbolic systems of conservation laws in one space variable can be treated in a formal manner. The possibility of focusing shows that total variation norm is not bounded, therefore no TVD schemes can exist for nonscalar hyperbolic systems in more than one space variable, linear or nonlinear. The positivity principle introduced in [7] is proper for multidimensional systems. The rationale of it is that in a formal sense positive schemes are l^2 stable.

The family of positive schemes constructed in [7] are simple, robust, fast, and low cost. The purpose of this paper is to present further applications of these methods.

In Riemann problems for two-dimensional gas dynamics the initial data are constant in each quadrant, so restricted that only one elementary wave, a one-dimensional shock, a one-dimensional rarefaction, or a two-dimensional slip line (a contact discontinuity) appears at each interface. This problem has been studied by many people in the last few years. Zhang and Zheng [13] predicted that there are a total of 16 genuinely different classes of Riemann problems for polytropic gas. Schulz-Rinne [8] proved one of them is impossible, and Schulz-Rinne, Collins, and Glaz [9] calculated all 15 solutions with a MUSCL-type scheme [2]. Recently Zhang, Chen, and Yang [14] pointed out that when two initially parallel slip lines are present, it makes a difference whether the vorticities generated have the same or opposite sign. In this paper we classify, similarly to [14], a total of 19 genuinely different solutions for polytropic gas; we compute all solutions.

The organization of this paper is as follows. In section 2 we describe the positivity principle, the family of positive schemes used here, including the FORTRAN 77 code. In section 3 we describe the Riemann problems. In section 4 we describe the numerical solutions obtained by our scheme. In section 5 we discuss the numerical results.

*Received by the editors September 13, 1995; accepted for publication (in revised form) April 29, 1996.

http://www.siam.org/journals/sisc/19-2/29181.html

†Courant Institute of Mathematical Sciences, 251 Mercer Street, New York, NY 10012 (lax@best.nyu.edu, xliu@cims.nyu.edu). The research of the first author was supported in part by Applied Mathematical Sciences Program of the U.S. Department of Energy under contract DE-FG02-88ER25053. The research of the second author was supported in part by National Science Foundation grants DMS-9112654 and DMS-9406467, and Air Force grant AFOSR F49620-94-1-0132.

2. Positive schemes.

2.1. Positivity principle. We consider multidimensional hyperbolic systems of conservation laws

$$U_t + \sum_{s=1}^{d} F_s(U)_{x_s} = 0, \tag{1}$$

where $U = (u_1, \ldots, u_n)^T \in \mathbf{R^n}$ and $x = (x_1, x_2, \ldots, x_d) \in \mathbf{R^d}$. We assume that all Jacobian matrices $A_s = \bigtriangledown F_s$ are symmetric. We construct a uniform Cartesian grid $\{\Omega_J\}$ in $\mathbf{R^d}$, where $J = (j_1, j_2, \ldots, j_d)$ is a lattice point in which all j_s are integers. In this uniform grid we denote cell averages as $U_J = \frac{1}{|\Omega|}\int_{\Omega_J} U(x,t)\,dx$, where $|\,\Omega\,|$ is the volume of the cell Ω_J.

Conservative schemes are of the form

$$U_J^* = U_J - \sum_{s=1}^{d} \frac{\Delta t}{\Delta x_s}[F_{J+1/2e_s} - F_{J-1/2e_s}], \tag{2}$$

where Δt is the time step and Δx_s is the spatial step in the x_s dimension.

Positivity principle. We call the conservative schemes (2) *positive* if we can rewrite the right side of (2) as

$$U_J^* = \sum_K C_K U_{J+K}, \tag{3}$$

so that the coefficient matrices C_K, which may themselves depend on all the U_{J+K} that occur in (2), have the following properties:

(i) each C_K is symmetric;

(ii) each C_K is positive, i.e., $C_K \geq 0$;

(iii) $\sum_K C_K = I$;

(iv) $C_K = 0$ except for a finite set of K.

Note that since the right side of (2) is a nonlinear function of the U_{J+K}, there are many ways of writing it in form (3).

As stated, the positivity principle applies only to (1), which is symmetric in the sense that the gradient A_s of the fluxes F_s are symmetric matrices. The gas dynamics equations treated here are not symmetric when written in terms of mass, momentum, and energy; however, they are symmetrizable in the sense that the matrices A_s can be made symmetric by the same similarity transformation. The positivity principle for such systems is that the C_K can be made simultaneously symmetric and positive at each point of phase space.

2.2. Construction of positive schemes. In [7] we have constructed a two-parameter family of second-order accurate positive schemes. The numerical flux $F_{j+1/2}^{num}$ in each coordinate direction was given by the following formula:

$$F_{j+1/2}^{num} = \frac{F(U_j) + F(U_{j+1})}{2} - \frac{1}{2}R[\alpha \mid \Lambda \mid (I - \Phi^0) + \beta\,\mathrm{diag}(\mu^i)(I - \Phi^1)]R^{-1}(U_{j+1} - U_j). \tag{4}$$

Here R is the matrix whose columns are the normalized right eigenvectors of A, the Roe matrix satisfying

$$F(U_{j+1}) - F(U_j) = A(U_{j+1} - U_j), \qquad A = A(U_j, U_{j+1});$$

R^{-1} is then the matrix whose rows are the normalized left eigenvectors l^k of A. $\mid \Lambda \mid = \operatorname{diag}\left(\mid \lambda^k \mid\right)$ is a diagonal matrix whose diagonal entries are the absolute value of the eigenvalues λ^k of A, and each diagonal entry of diagonal matrix $\operatorname{diag}\left(\mu^k\right)$ satisfies $\mu^k \geq \mid \lambda^k \mid$. The parameters α and β satisfy $0 \leq \alpha \leq 1$ and $\alpha + \beta \geq 1$. $\Phi^0 = \operatorname{diag}\left(\phi_k^0(\theta^k)\right)$ and $\Phi^1 = \operatorname{diag}\left(\phi^1(\theta^k)\right)$ are diagonal matrices whose entries are limiter functions subject to

$$0 \leq \phi_k^0(\theta) \leq 2, \qquad 0 \leq \phi_k^0(\theta)/\theta \leq 2, \qquad \phi_k^0(1) = 1,$$

and

$$0 \leq \phi^1(\theta) \leq 1, \qquad 0 \leq \phi^1(\theta)/\theta \leq 1, \qquad \phi^1(1) = 1,$$

respectively, where each ϕ_k^0 could be different for each k and ϕ^1 is the minmod limiter function. Each argument θ^k of the limiter function ϕ is defined as

$$\theta^k = \frac{l^k(U_{j'+1} - U_{j'})}{l^k(U_{j+1} - U_j)}, \qquad 1 \leq k \leq n, \qquad \text{where } j' = \begin{cases} j-1 & \text{if} \quad \lambda^k \geq 0, \\ j+1 & \text{otherwise.} \end{cases}$$

The schemes (2) and (4) are positive under the following CFL condition:

$$\sum_{s=1}^{d} \frac{\Delta t}{\Delta x_s} \left(\alpha_s \max_{1 \leq i \leq n, U} \mid \lambda^{s,i} \mid + \beta_s \max_{1 \leq i \leq n, U} \mu^{s,i} \right) \leq \frac{1}{2}.$$

We write out (4) more fully:

$$\begin{aligned} F_{j+1/2}^{num} &= \frac{F(U_j) + F(U_{j+1})}{2} \\ &\quad -\frac{1}{2} R \operatorname{diag}\left(\alpha \mid \lambda^k \mid (1 - \phi_k^0(\theta^k)) + \beta \mu^k (1 - \phi^1(\theta^k))\right) \begin{pmatrix} l^1(U_{j+1} - U_j) \\ \vdots \\ l^n(U_{j+1} - U_j) \end{pmatrix} \\ &= \frac{F(U_j) + F(U_{j+1})}{2} \\ &\quad + R \begin{pmatrix} -\frac{1}{2}\left(\alpha \mid \lambda^1 \mid (1 - \phi_1^0(\theta^1)) + \beta \mu^1 (1 - \phi^1(\theta^1))\right) l^1(U_{j+1} - U_j) \\ \vdots \\ -\frac{1}{2}\left(\alpha \mid \lambda^n \mid (1 - \phi_n^0(\theta^n)) + \beta \mu^n (1 - \phi^n(\theta^n))\right) l^n(U_{j+1} - U_j) \end{pmatrix} \\ &= \frac{F(U_j) + F(U_{j+1})}{2} \\ &\quad + R \begin{pmatrix} -\frac{1}{2}\left(\alpha \mid \lambda^1 \mid (1 - \phi_1^0(\theta^1)) + \beta \mu^1 (1 - \phi^1(\theta^1))\right) dw^1 \\ \vdots \\ -\frac{1}{2}\left(\alpha \mid \lambda^n \mid (1 - \phi_n^0(\theta^n)) + \beta \mu^n (1 - \phi^n(\theta^n))\right) dw^n \end{pmatrix} \\ &= \frac{F(U_j) + F(U_{j+1})}{2} + R \begin{pmatrix} dwf^1 \\ \vdots \\ dwf^n \end{pmatrix}, \end{aligned} \tag{5}$$

where $dw^k = l^k(U_{j+1} - U_j)$ and $dwf^k = -\frac{1}{2}(\alpha \mid \lambda^k \mid (1 - \phi_k^0(\theta^k)) + \beta\mu^k(1 - \phi^k(\theta^k)))dw^k$.

The positive schemes (2), (4) are second-order accurate in space and first order in time. We then use the second-order accurate energy-preserving Runge–Kutta method of Shu [10] and Shu and Osher [11] to achieve second-order accuracy in time: for $m = 0, 1, \ldots,$

$$
\begin{aligned}
U_J^* &= U_J^m - \sum_{s=1}^{d} \tfrac{\Delta t}{\Delta x_s}[F_{J+1/2e_s} - F_{J-1/2e_s}],\\
U_J^{**} &= U_J^* - \sum_{s=1}^{d} \tfrac{\Delta t}{\Delta x_s}[F^*_{J+1/2e_s} - F^*_{J-1/2e_s}],\\
U_J^{m+1} &= \tfrac{1}{2}U_J^m + \tfrac{1}{2}U_J^{**}.
\end{aligned}
$$

Remark 1. For two dimensions an alternative to achieve second-order accuracy both in space and time is to use one-dimensional positive schemes based on the Lax–Wendroff flux [7]

$$
\begin{aligned}
F^{num}_{j+1/2} &= \frac{F(U_j) + F(U_{j+1})}{2}\\
&\quad -\frac{1}{2}R\left[\alpha \mid \Lambda \mid (I - \Phi^0) + \beta\,\mathrm{diag}(\mu^i)(I - \Phi^1) + \frac{\Delta t}{\Delta x}\Lambda^2\right] R^{-1}(U_{j+1} - U_j)
\end{aligned}
\tag{6}
$$

combined with Strang's second-order accurate dimension-by-dimension splitting [12]. There are three advantages of doing that: (1) The Strang's splitting is energy preserving if the one-dimensional schemes are. (2) The Strang's splitting guarantees that the resulting combined schemes have second-order accuracy if the one-dimensional schemes do; hence the combined schemes are second-order accurate both in space and time. Therefore, there is no need to do two-stage Runge–Kutta, which saves at least half of the cost. (3) The Strang's splitting also guarantees that the combined schemes have the same CFL number as that of the combined one-dimensional schemes. Therefore, the positive schemes (6) combined with Strang's splitting have the CFL number $\sqrt{2} - 1$. Note that the CFL number of the positive schemes (4) combined with Runge–Kutta is $\frac{1}{4}$ in general for two dimensions.

Remark 2. It is well known that the Roe scheme admits entropy violating solutions because the diffusive term of the Roe scheme in each field is $-\frac{1}{2} \mid \lambda^k \mid dw^k$, which is zero at zero eigenvalue $\lambda^k = 0$ field. The diffusive term of the positive flux (4) in each field is $-\frac{1}{2}[\alpha \mid \lambda^k \mid (1 - \phi^0) + \beta\mu^k(1 - \phi^1)]dw^k$. At the zero eigenvalue field we construct a nonzero diffusive term by choosing μ^k and β larger than zero. Therefore, the positive schemes always can be constructed to have enough dissipation to avoid entropy violating solutions.

The flow chart of the above procedure (5) can be described in FORTRAN 77 as follows:

```
Evaluate R, R^{-1}, Λ from U_j and U_{j+1}
do k = 1, n
   dw^k = l^k(U_{j+1} - U_j)
   if (λ^k ≥ 0) then
      dwup = l^k(U_j - U_{j-1})
   else
      dwup = l^k(U_{j+2} - U_{j+1})
```

end if
Evaluate $\phi_k^0(\theta^k)$ and $\phi^1(\theta^k)$ from $\theta^k = dwup/dw^k$
$dwf^k = -\frac{1}{2}\left(\alpha \mid \lambda^k \mid (1-\phi_k^0(\theta^k)) + \beta\mu^k(1-\phi^1(\theta^k))\right) dw^k$
end do
$F_{j+1/2} = \frac{F(U_j)+F(U_{j+1})}{2} + R \cdot dwf$

In the following we present FORTRAN 77 code (excluding the initial and boundary subroutines) of positive scheme for solving two-dimensional gas dynamics in a rectangular grid.

Positive schemes.

```
c**************************************************************************
c
c   Program: positive
c
c    Object: Using 2nd order accurage positive schemes to solve
c            2-D gas dynamics problems
c
c Variables: U=(ul,u2,u3,u4)^T  Conservative Variables
c            ul=rho             Density
c            u2=m               Momentum in x direction
c            u3=n               Momentum in y direction
c            u4=e               Total energy
c
c**************************************************************************
c
     program positive
     implicit  real*8 (a-h,m-z)
     parameter  (lmx=400,lmy=400)
     common /gridI/lx,ly,lsteps
     common /gridR/T,dt,dx,dy,xlambda,ylambda
     dimension U(4,-1:lmx+3,-1:lmy+3),Ul(4,-1:lmx+3,-1:lmy+3)
     call grid_para
     call initial(U)
     do l=1,lsteps
       call evolve(U,Ul)
       call bdy(Ul)
       call evolve(Ul,Ul)
       do j=1,ly+1
         do i=1,lx+1
           do k=1,4
             U(k,i,j)=0.5d0*(U(k,i,j)+Ul(k,i,j))
           end do
         end do
       end do
       call bdy(U)
     end do
     open(10,file='rho.mat',status='unknown')
     write(10,2000) T,dt,dt/dx,lx,ly
     write(10,1000) ((U(1,i,j),j=1,ly+1),i=1,lx+1)
1000 format(f9.4,f9.4,f9.4,f9.4,f9.4)
2000 format(f9.4,f9.4,f9.4,i5,i5)
     stop
     end
c**************************************************************************
c
c  Subroutine: Evolve
c
c      Object: To evaluate the future values: rhol,ml,nl,el
c              from the current values:       rho, m, n, e
```

```
c
c   Variables: up                U_{j+l}
c              um                U_{j}
c              dup               U_{j+2}-U_{j+l}
c              dum               U_{j}-U_{j-l}
c              du                U_{j+l}-U_{j}
c              dw                R^{-l}*(U_{j+l}-U_{j})
c              dwf               Diffusive flux in char fields
c
c              fc                Central differencing flux
c              df=R*dwf          Diffusive flux
c              f=fc+df           Flux in x direction
c              g                 Flux in y direction
c
c**********************************************************************
c
        subroutine evolve (U,Ul)
        implicit real*8 (a-h,m-z)
        common /gridI/lx,ly,lsteps
        common /gridR/T,dt,dx,dy,xlambda,ylambda
        parameter (lmx=400,lmy=400)
        dimension U(4,-l:lmx+3,-l:lmy+3),Ul(4,-l:lmx+3,-l:lmy+3)
        dimension up(4), um(4),du(4),dup(4),dum(4)
        dimension fc(4),df(4),f(4,0:lmx+l,0:1my+l),g(4,0:lmx+l,0:lmy+l)
        do j=l,ly+l
          do i=0,lx+l
            do k=l,4
              up(k)=U(k,i+l,j)
              um(k)=U(k,i,j)
              dum(k)=U(k,i,j)-U(k,i-l,j)
              dup(k)=U(k,i+2,j)-U(k,i+l,j)
              du(k)=U(k,i+l,j)-U(k,i,j)
            end do
            call central(up,um,fc)
            call diffusiveflux(up,um,du,dup,dum,df)
            do k=l,4
              f(k,i,j)=fc(k)+df(k)
            end do
          end do
        end do

        do j=0,ly+l
          do i=l,lx+l
            do k=l,4
              kl=k
              if(k.eq.2)kl=3
              if(k.eq.3)kl=2
              up(k)=U(kl,i,j+l)
              um(k)=U(kl,i,j)
              dum(k)=U(kl,i,j)-U(kl,i,j-l)
              dup(k)=U(kl,i,j+2)-U(kl,i,j+l)
              du(k)=U(kl,i,j+l)-U(kl,i,j)
            end do
            call central(up,um,fc)
            call diffusiveflux(up,um,du,dup,dum,df)
            do k=l,4
              kl=k
              if(k.eq.2)kl=3
              if(k.eq.3)kl=2
              g(k,i,j)=fc(kl)+df(kl)
            end do
          end do
        end do
```

```
do j=1,ly+1
  do i=1,1x+1
    do k=1,4
      Ul(k,i,j)=U(k,i,j)-xlambda*(f(k,i,j)-f(k,i-1,j))
c                        -ylambda*(g(k,i,j)-g(k,i,j-1))
    end do
  end do
end do
return
end
c**************************************************************************
c
c Subroutine: eigs
c
c     Object: To calculate the right eigenvector matrx, the left
c             eigenvector matrx and eigenvalues of Roe matrix
c             A=A(U_{j+1},U_{j}), where F(U_{j+1})-F(U_{j})-
c             A(U_{j+1},U_{j})*(U_{j+1}-U_{j})
c
c Variables:  up                U_{j+1}
c             um                U_{j}
c             r                 Right eigenvector matrix R of the A
c             ri                Left eigenvector matrix R^{-1} of the A
c             eig               Eigenvalues of the A
c
c
c**************************************************************************
c
    subroutine eigs(up,um,r,ri,eig)
    implicit real*8 (a-h,m-z)
    parameter (gamma=1.4d0)
    dimension up(4),um(4),r(4,4),ri(4,4),eig(4)
    ul=um(2)/um(1)
    vl=um(3)/um(1)
    Hl=(um(4)+(gamma-1.0d0)*(um(4)-0.5d0*(ul*ul+vl*vl)*um(1)))/um(1)
    u2=up(2)/up(1)
    v2=up(3)/up(1)
    H2=(up(4)+(gamma-1.0d0)*(up(4)-0.5d0*(u2*u2+v2*v2)*up(1)))/up(1)
    w1=dsqrt(um(1))+dsqrt(up(1))
    u=(dsqrt(um(1))*ul+dsqrt(up(1))*u2)/w1
    v=(dsqrt(um(1))*vl+dsqrt(up(1))*v2)/w1
    H=(dsqrt(um(1))*Hl+dsqrt(up(1))*H2)/w1
    q2=u*u+v*v
    c=dsqrt((gamma-1.0d0)*(H-0.5d0*q2))
    r(1,1)=1.0d0
    r(2,1)=u-c
    r(3,1)=v
    r(4,1)=H-u*c
    r(1,2)=0.0d0
    r(2,2)=0.0d0
    r(3,2)=1.0d0
    r(4,2)=v
    r(1,3)=1.0d0
    r(2,3)=u
    r(3,3)=v
    r(4,3)=0.5d0*q2
    r(1,4)=1.0d0
    r(2,4)=u+c
    r(3,4)=v
    r(4,4)=H+u*c
    b1=1.0d0/(H-0.5d0*q2)
    b2=0.5d0*q2*b1
    ri(1,1)=0.5d0*(b2+u/c)
```

```
    ri(1,2)=-0.5d0/c-0.5d0*bl*u
    ri(1,3)=-0.50*bl*v
    ri(1,4)=0.5d0*bl
    ri(2,1)=-v
    ri(2,2)=0.0d0
    ri(2,3)=1.0d0
    ri(2,4)=0.0d0
    ri(3,1)=1.0d0-b2
    ri(3,2)=bl*u
    ri(3,3)=bl*v
    ri(3,4)=-bl
    ri(4,1)=0.5d0*(b2-u/c)
    ri(4,2)=0.5d0/c-0.5d0*bl*u
    ri(4,3)=-0.5d0*bl*v
    ri(4,4)=0.5d0*bl
    eig(1)=u-c
    eig(2)=u
    eig(3)=u
    eig(4)=u+c
    return
    end

c**************************************************************************
c
c Subroutine: diffusiveflux
c
c     Object: To calculate the diffusive flux df
c
c  Variables: up                U_{j+1}
c             um                U_{j}
c             du                U_{j+1}-U{j}
c             dup               U_{j+2}-U{j+1}
c             dum               U_{j}-U_{j-1}
c             df                Diffusive flux
c             dw                R^{-1}*(U_{j+1}-U{j})
c             dwf               Diffusive flux in char form
c             r                 Right eigenvector matrix R of the A
c             ri                Left eigenvector matrix R^{-1} fo the A
c             eig               Eigenvalues of the A
c
c**************************************************************************
c
     subroutine diffusiveflux(up,um,du,dup,dum,df)
     implicit real*8 (a-h,m-z)
     common /para/alpha,beta
     dimension up(4),um(4),du(4),dup(4),dum(4),df(4)
     dimension dw(4),dwf(4),r(4,4),ri(4,4),eig(4)
     call eigs(up,um,r,ri,eig)
     mu-dmaxl(dabs(eig(1)),dabs(eig(4)))
     do k=1,4
       dw(k)=ri(k,1)*du(1)+ri(k,2)*du(2)+ri(k,3)*du(3)+ri(k,4)*du(4)
       dwup=ri(k,1)*dup(1)+ri(k,2)*dup(2)+ri(k,3)*dup(3)+ri(k,4)*dup(4)
       if(eig(k).ge.0.0d0)then
       dwup=ri(k,1)*dum(1)+ri(k,2)*dum(2)+ri(k,3)*dum(3)+ri(k,4)*dum(4)
       end if
       call limiter(dw(k),dwup,phi0,phi1,k)
       dwf(k)=-0.5d0*(alpha*(1.0d0-phi0)*dabs(eig(k))
     c               +beta*(1.0d0-phi1)*mu)*dw(k)
      end do
      do k=1,4
        df(k)=r(k,1)*dwf(1)+r(k,2)*dwf(2)+r(k,3)*dwf(3)+r(k,4)*dwf(4)
      end do
```

```
     return
     end
c**********************************************************************
c
c Subroutine:  limiter
c
c     Object: To evaluate two limiters phi^0 and phi^l from
c             theta=dw/dwup
c
c  Variables: phi0               Limiter in the least dissipative flux
c             phil               Limiter in the more dissipative flux
c             dw                 R^{-l}*(U_{j+l}-U_{j})
c             dwup               R^{-l}*(U_{j+2}-U_{j+l}) if eig<0, or
c                                R^{-l}*(U_{j}-U_{j-l})   otherwise
c
c**********************************************************************
c
       subroutine limiter(dw,dwup,phi0,phil,k)
       implicit real*8 (a-h,m-z)
c--------Superbee------------------------------------------------------
       phi0=0.0d0
       if(dw.eq.0.0d0.and.dwup.gt.0.0d0)phi0=2.0d0
       if(dw*dwup.gt.0.0d0)then
         theta=dwup/dw
         if(theta.le.0.5d0)then
           phi0=2.0d0*theta
         else if(theta.le.1.0d0.and.theta.gt.0.5d0)then
           phi0=1.0d0
         else if(theta.le.2.0d0.and.theta.gt.1.0d0)then
           phi0=theta
         else
           phi0=2.0d0
         end if
       end if
 c-------VanLeer------------------------------------------------------
       phi=0.0d0
       if(dw.eq.0.0d0.and.dwup.gt.0.0d0)phi=2.0d0
       if(dw*dwup.gt.0.0d0)then
         theta=dwup/dw
         phi=2.0d0*theta/(1.0d0+theta)
       end if
 c-------MinMod-------------------------------------------------------
       phil=0.0d0
       if(dw.eq.0.0d0.and.dwup.gt.0.0d0)phil=1.0d0
       if(dw*dwup.gt.0.0d0)then
         phil=1.0d0
         if(dwup/dw.le.1.0d0)then
           phil=dwup/dw
         end if
       end if
 c----------------------------------------------------------------------
       if(k.eq.1.or.k.eq.4)then
         phi0=phi
       end if
       return
       end
 c**********************************************************************
 c
 c Subroutine: central
 c
 c     Object: To calculate the central differencing flux
 c
```

```
c Variables: fc=0.5d0*(F(U_{j+1})+F(U_{j}))
c
c**********************************************************************
c
      subroutine central(up,um,fc)
      implicit real*8 (a-h,m-z)
      parameter (gamma=1.4d0)
      dimension up(4),um(4),fc(4)
      pl=(gamma-1.0d0)*(um(4)-0.5d0*(um(2)**2+um(3)**2)/um(1))
      pr=(gamma-1.0d0)*(up(4)-0.5d0*(up(2)**2+up(3)**2)/up(1))
      fc(1)=0.5d0*(um(2)+up(2))
      fc(2)=0.5d0*(um(2)**2/um(1)+pl+up(2)**2/up(1)+pr)
      fc(3)=0.5d0*(um(2)*um(3)/um(1)+up(2)*up(3)/up(1))
      fc(4)=0.5d0*((um(4)+pl)*um(2)/um(1)+(up(4)+pr)*up(2)/up(1))
      return
      end
c**********************************************************************
c
c Subroutine: grid_para
c
c     Object: 1) To setup grid for the computing domain [0,1]X[0,1] in R^2
c             and time interval [0,T]
c             2) To setup parameters \alpha and \beta
c
c  Variables: lx                number of grid points in x direction
c             ly                number of grid points in y direction
c             lsteps            number of time steps
c             T                 stopping time T
c             dt                time step
c             dx                stepsize in x direction
c             dy                stepsize in y direction
c
c**********************************************************************
c
      subroutine grid_para
      implicit real*8 (a-h,m-z)
      common /gridI/lx,ly,lsteps
      common /gridR/T,dt,dx,dy,xlambda,ylambda
      common /para/alpha,beta
      write(*,*) ' Enter the Number of Grid Points in x direction '
      read(*,*) lx
      write(*,*) ' Enter the Number of Grid Points in y direction '
      read(*,*) ly
      dx=1.0d00/dble(lx)
      dy=1.0d00/dble(ly)
      write(*,*) 'Enter Stopping Time, T:'
      read(*,*) T
      write(*,*) 'Enter the minmum of dt/dx and dt/dy:'
      read(*,*) xlambda
      dt=xlambda*dy
      if(xlambda*dx.lt.xlambda*dy)dt=xlambda*dx
      if(T/dt.gt.dble(dint(T/dt)))then
        lsteps=dint(T/dt)+1
      else
        lsteps=dint(T/dt)
      endif
      if(T.eq.0.0d00)then
        dt=0.0d00
      else
        dt=T/dble(lsteps)
      end if
      xlambda=dt/dx
      ylambda=dt/dy
```

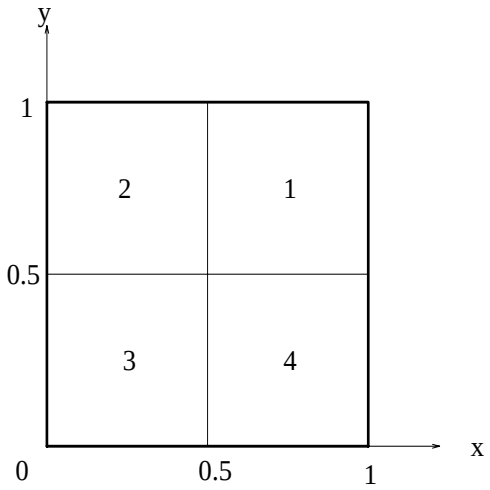

FIG. 0.

```
write(*,*) 'Enter the parameters alpha= and beta='
read(*,*) alpha,beta
write(*,*) 'the number of timesteps : ',lsteps
write(*,*) 'Running..... '
return
end
```

2.3. Features of the positive schemes. The first advantage is its great simplicity. We evaluate the flux dimension-by-dimension, far simpler than any genuinely multidimensional approach. The positive flux evaluating procedure only involves very simple algebraic operators.

The second advantage is its very low cost. To evaluate one flux the positive scheme needs three matrix–vector multiplications. The first is $R^{-1}(U_{j+1} - U_j)$, the second is $l^k(U_{j'+1} - U_{j'})$ for $k = 1, \ldots, n$, and the third is $R \cdot dwf$. Any scheme using characteristic decomposition, in general, needs at least two matrix–vector multiplications. Only simple and few algebraic operations are involved, and hence the scheme runs fast.

The third advantage is its robustness. Positive schemes have many parameters which give much flexibility in solving different problems with high resolution. However, we can fix the parameters and still obtain high resolution for many problems, i.e., the positive schemes are able to obtain high resolution without fine tuning.

3. The Riemann problem for two-dimensional gas dynamics. In the Riemann problems for two-dimensional gas dynamics the initial data are constant in each quadrant (see Figure 0) and so restricted that only one elementary wave, a one-dimensional shock, a one-dimensional rarefaction wave, or a two-dimensional slip line (contact discontinuity) appears at each interface.

We consider the Euler equations for a compressible gas,

$$U_t + F(U)_x + G(U)_y = 0, \tag{7}$$

where

$$U = \begin{pmatrix} \rho \\ \rho u \\ \rho v \\ e \end{pmatrix}, \qquad F = \begin{pmatrix} \rho u \\ \rho u^2 + p \\ \rho uv \\ u(e+p) \end{pmatrix}, \qquad G = \begin{pmatrix} \rho v \\ \rho uv \\ \rho v^2 + p \\ v(e+p) \end{pmatrix}. \tag{8}$$

Here ρ is the density, u is the velocity component in x-dimension, v is the velocity component in y-dimension, p is the pressure, and e is the energy. p, ρ, and e are connected by an equation of state that for an isentropic gas or a polytropic gas takes the form

$$p = A\rho^{\gamma}, \qquad e = \frac{p}{\gamma - 1} + \frac{\rho(u^2 + v^2)}{2}, \tag{9}$$

respectively; here $A > 0$ is a function of entropy.

The Riemann problem is the initial value problem for (7) with initial data

$$(p, \rho, u, v)(x, y, 0) = (p_i, \rho_i, u_i, v_i), \qquad i = 1, 2, 3, 4,$$

for compressible gas, where i denotes the ith quadrant.

We are studying two-dimensional Riemann problems where each planar wave at an interface connecting two neighboring constant initial states consists of a single elementary wave, i.e., a one-dimensional rarefaction wave, a one-dimensional shock wave, or a slip line, i.e., one with a discontinuous tangential velocity.

Here and below w represents velocity components perpendicular to the line of discontinuity, and $w^{'}$ represents velocity components parallel to it. At an interface $(l, r) \in \{(2,1), (3,2), (3,4), (4,1)\}$, a backward $\overleftarrow{R_{lr}}$ or forward rarefaction wave $\overrightarrow{R_{lr}}$ is described by the formula

$$\overleftarrow{R_{lr}}: \qquad w_l - w_r = \frac{2\sqrt{\gamma}}{\gamma - 1}\left(\sqrt{\frac{p_r}{\rho_r}} - \sqrt{\frac{p_l}{\rho_l}}\right), \qquad w_l^{'} = w_r^{'}, \tag{10}$$

or

$$\overrightarrow{R_{lr}}: \qquad w_l - w_r = \frac{2\sqrt{\gamma}}{\gamma - 1}\left(\sqrt{\frac{p_l}{\rho_l}} - \sqrt{\frac{p_r}{\rho_r}}\right), \qquad w_l^{'} = w_r^{'}. \tag{11}$$

For a polytropic gas

$$\overleftarrow{R_{lr}} \quad \text{and} \quad \overrightarrow{R_{lr}}: \qquad \frac{p_l}{p_r} = \left(\frac{\rho_l}{\rho_r}\right)^{\gamma}. \tag{12}$$

A backward $\overleftarrow{S_{lr}}$ or forward shock wave $\overrightarrow{S_{lr}}$ is described by the formula

$$\overleftarrow{S_{lr}}: \qquad \frac{w_r - w_l}{\rho_r - \rho_l} = -\sqrt{\frac{1}{\rho_r \rho_l}\frac{p_r - p_l}{\rho_r - \rho_l}}, \qquad w_l^{'} = w_r^{'}, \tag{13}$$

or

$$\overrightarrow{S_{lr}}: \qquad \frac{w_r - w_l}{\rho_r - \rho_l} = +\sqrt{\frac{1}{\rho_r \rho_l}\frac{p_r - p_l}{\rho_r - \rho_l}}, \qquad w_l^{'} = w_r^{'}. \tag{14}$$

For a polytropic gas

$$\overleftarrow{S_{lr}} \quad \text{and} \quad \overrightarrow{S_{lr}}: \qquad \frac{\rho_l}{\rho_r} = \left(\frac{p_l}{p_r} + \frac{\gamma - 1}{\gamma + 1}\right) \Bigg/ \left(1 + \frac{(\gamma - 1)p_l}{(\gamma + 1)p_r}\right). \tag{15}$$

In two dimensions a negative J_{lr}^{-} or positive slip line J_{lr}^{+} (a contact discontinuity) is described by the formula

$$J_{lr}^{-}: \qquad w_l = w_r, \quad p_l = p_r, \quad w_l^{'} \geq w_r^{'}, \tag{16}$$

TABLE 1.

$4R$:	$\overrightarrow{R_{32}}$	$\overrightarrow{R_{21}}$ $\overrightarrow{R_{41}}$ $\overrightarrow{R_{34}}$	$\overleftarrow{R_{32}}$	$\overrightarrow{R_{21}}$ $\overrightarrow{R_{41}}$ $\overleftarrow{R_{34}}$								
$4S$:	$\overleftarrow{S_{32}}$	$\overleftarrow{S_{21}}$ $\overleftarrow{S_{41}}$ $\overleftarrow{S_{34}}$	$\overrightarrow{S_{32}}$	$\overleftarrow{S_{21}}$ $\overleftarrow{S_{41}}$ $\overrightarrow{S_{34}}$								
$4J$:	J_{32}^{-}	J_{21}^{-} J_{41}^{-} J_{34}^{-}	J_{32}^{+}	J_{21}^{-} J_{41}^{+} J_{34}^{-}								
$2J+2R$:	J_{32}^{-}	$\overrightarrow{R_{21}}$ $\overrightarrow{R_{41}}$ J_{34}^{-}	J_{32}^{-}	$\overleftarrow{R_{21}}$ $\overleftarrow{R_{41}}$ J_{34}^{-}	$\overrightarrow{R_{32}}$	J_{21}^{+} $\overrightarrow{R_{41}}$ J_{34}^{+}	$\overrightarrow{R_{32}}$	J_{21}^{-} $\overrightarrow{R_{41}}$ J_{34}^{+}				
$2J+2S$:	J_{32}^{+}	$\overleftarrow{S_{21}}$ $\overleftarrow{S_{41}}$ J_{34}^{+}	J_{32}^{+}	$\overrightarrow{S_{21}}$ $\overrightarrow{S_{41}}$ J_{34}^{+}	$\overleftarrow{S_{32}}$	J_{21}^{-} $\overleftarrow{S_{41}}$ J_{34}^{-}	$\overleftarrow{S_{32}}$	J_{21}^{+} $\overleftarrow{S_{41}}$ J_{34}^{-}				
$2J+R+S$:	J_{32}^{-}	$\overrightarrow{R_{21}}$ $\overleftarrow{S_{41}}$ J_{34}^{+}	J_{32}^{-}	$\overleftarrow{R_{21}}$ $\overrightarrow{S_{41}}$ J_{34}^{+}	$\overleftarrow{S_{32}}$	J_{21}^{-} $\overrightarrow{R_{41}}$ J_{34}^{-}	$\overleftarrow{S_{32}}$	J_{21}^{+} $\overrightarrow{R_{41}}$ J_{34}^{+}	$\overleftarrow{S_{32}}$	J_{21}^{+} $\overrightarrow{R_{41}}$ J_{34}^{-}		

or

$$J_{lr}^{+}: \qquad w_l = w_r, \quad p_l = p_r, \quad w_l^{'} \le w_r^{'}. \tag{17}$$

The total number of genuinely different configurations for polytropic gas is 19; see Table 1.

Remark 3. According to [9] the total number of genuinely different configurations for polytropic gas is 15, if we ignore the difference between positive slips and negative ones. Our calculations show that the sign of the slip makes a difference in the resulting flow pattern.

1. The configuration $\overrightarrow{R_{32}}$ J_{21} J_{34} $\overrightarrow{R_{41}}$ in [9] includes two distinct cases:

   (a) $\overrightarrow{R_{32}}$ J_{21}^{+} J_{34}^{+} $\overrightarrow{R_{41}}$, (b) $\overrightarrow{R_{32}}$ J_{21}^{-} J_{34}^{-} $\overrightarrow{R_{41}}$, (c) $\overrightarrow{R_{32}}$ J_{21}^{-} J_{34}^{+} $\overrightarrow{R_{41}}$, and

   (d) $\overrightarrow{R_{32}}$ J_{21}^{+} J_{34}^{-} $\overrightarrow{R_{41}}$.

   (a) and (b) are the same, as are (c) and (d), respectively.

2. The configuration $\overleftarrow{S_{32}}$ J_{21} J_{34} $\overleftarrow{S_{41}}$ in [9] includes two distinct cases:

   (a) $\overleftarrow{S_{32}}$ J_{21}^{-} J_{34}^{-} $\overleftarrow{S_{41}}$, (b) $\overleftarrow{S_{32}}$ J_{21}^{+} J_{34}^{+} $\overleftarrow{S_{41}}$, (c) $\overleftarrow{S_{32}}$ J_{21}^{-} J_{34}^{+} $\overleftarrow{S_{41}}$, and

   (d) $\overleftarrow{S_{32}}$ J_{21}^{-} J_{34}^{+} $\overleftarrow{S_{41}}$.

   (a) and (b) are the same, as are (c) and (d), respectively.

3. The configuration $\overleftarrow{S_{32}}$ $\begin{matrix} J_{21} \\ J_{34} \end{matrix}$ $\overrightarrow{R_{41}}$ in [9] includes three distinct cases:
   (a) $\overleftarrow{S_{32}}$ $\begin{matrix} J_{21}^- \\ J_{34}^- \end{matrix}$ $\overrightarrow{R_{41}}$, (b) $\overleftarrow{S_{32}}$ $\begin{matrix} J_{21}^+ \\ J_{34}^+ \end{matrix}$ $\overrightarrow{R_{41}}$, (c) $\overleftarrow{S_{32}}$ $\begin{matrix} J_{21}^- \\ J_{34}^+ \end{matrix}$ $\overrightarrow{R_{41}}$, and
   (d) $\overleftarrow{S_{32}}$ $\begin{matrix} J_{21}^- \\ J_{34}^+ \end{matrix}$ $\overrightarrow{R_{41}}$.
   (c) is impossible because J_{21}^-, $\overleftarrow{S_{32}}$, J_{34}^+, and $\overrightarrow{R_{41}}$ require that $v_2 > v_1$, $v_3 > v_2$, $v_3 < v_4$, and $v_4 < v_1$, respectively, which is a contradiction. (a) and (b) are different.
4. The rest of the configurations in Table 1 are exactly the same as the ones in [8].
5. The above reasoning does not involve any additional conditions (12) and (15) of polytropic gas, hence they also work for isentropic gas. Therefore, those configurations are the possible configurations for isentropic gas.

4. Numerical experiments. In this section we give out initial data for all configurations for a polytropic gas; fifteen of those initial data are the same as ones given in [9].

In all of our numerical experiments we use the same parameters $\alpha = 0.9$, $\beta = 0.1$, and vanLeer's limiter for $\phi_k^0(\theta^k)$ as the ones used for oblique shock and step problems in [7]. The accompanying figures show density contour lines.

CONFIGURATION 1. $\overrightarrow{R_{32}}$ $\begin{matrix} \overrightarrow{R_{21}} \\ \overrightarrow{R_{34}} \end{matrix}$ $\overrightarrow{R_{41}}$: the initial data are

$p_2 = 0.4$	$\rho_2 = 0.5197$	$p_1 = 1$	$\rho_1 = 1$
$u_2 = -0.7259$	$v_2 = 0$	$u_1 = 0$	$v_1 = 0$
$p_3 = 0.0439$	$\rho_3 = 0.1072$	$p_4 = 0.15$	$\rho_4 = 0.2579$
$u_3 = -0.7259$	$v_3 = -1.4045$	$u_4 = 0$	$v_4 = -1.4045$

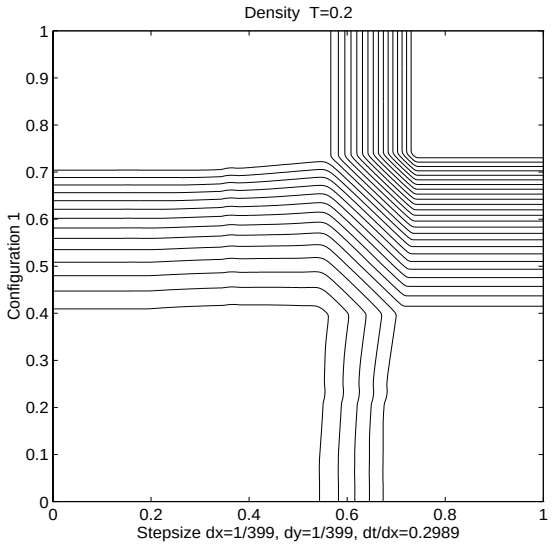

FIG. 1

CONFIGURATION 2. $\overleftarrow{R_{32}}$ $\begin{matrix} \overrightarrow{R_{21}} \\ \overleftarrow{R_{34}} \end{matrix}$ $\overrightarrow{R_{41}}$: the initial data are

$p_2 = 0.4$	$\rho_2 = 0.5197$	$p_1 = 1$	$\rho_1 = 1$
$u_2 = -0.7259$	$v_2 = 0$	$u_1 = 0$	$v_1 = 0$
$p_3 = 1$	$\rho_3 = 1$	$p_4 = 0.4$	$\rho_4 = 0.5197$
$u_3 = -0.7259$	$v_3 = -0.7259$	$u_4 = 0$	$v_4 = -0.7259$

CONFIGURATION 3. $\overleftarrow{S_{32}}$ $\overleftarrow{S_{21}}$ $\overleftarrow{S_{41}}$ $\overleftarrow{S_{34}}$: the initial data are

$p_2 = 0.3$	$\rho_2 = 0.5323$	$p_1 = 1.5$	$\rho_1 = 1.5$
$u_2 = 1.206$	$v_2 = 0$	$u_1 = 0$	$v_1 = 0$
$p_3 = 0.029$	$\rho_3 = 0.138$	$p_4 = 0.3$	$\rho_4 = 0.5323$
$u_3 = 1.206$	$v_3 = 1.206$	$u_4 = 0$	$v_4 = 1.206$

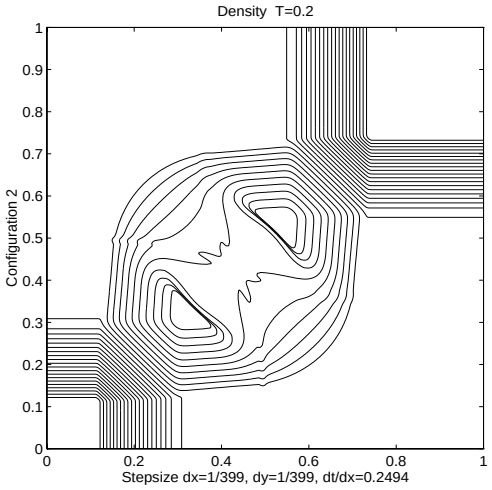

FIG. 2

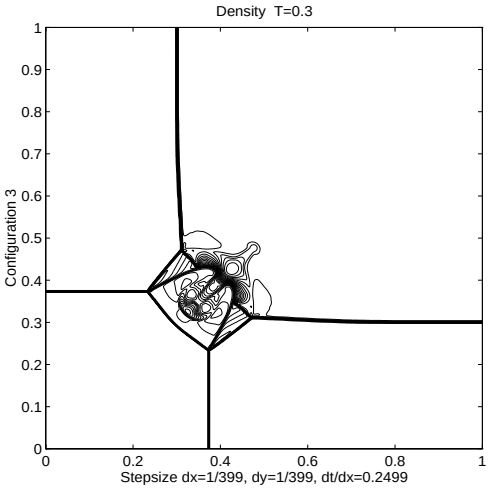

FIG. 3

CONFIGURATION 4. $\overrightarrow{S_{32}}$ $\overleftarrow{S_{21}}$ $\overleftarrow{S_{41}}$ $\overrightarrow{S_{34}}$: the initial data are

$p_2 = 0.35$	$\rho_2 = 0.5065$	$p_1 = 1.1$	$\rho_1 = 1.1$
$u_2 = 0.8939$	$v_2 = 0$	$u_1 = 0$	$v_1 = 0$
$p_3 = 1.1$	$\rho_3 = 1.1$	$p_4 = 0.35$	$\rho_4 = 0.5065$
$u_3 = 0.8939$	$v_3 = 0.8939$	$u_4 = 0$	$v_4 = 0.8939$

CONFIGURATION 5. J_{32}^- J_{21}^- J_{41}^- J_{34}^- : the initial data are

$p_2 = 1$	$\rho_2 = 2$	$p_1 = 1$	$\rho_1 = 1$
$u_2 = -0.75$	$v_2 = 0.5$	$u_1 = -0.75$	$v_1 = -0.5$
$p_3 = 1$	$\rho_3 = 1$	$p_4 = 1$	$\rho_4 = 3$
$u_3 = 0.75$	$v_3 = 0.5$	$u_4 = 0.75$	$v_4 = -0.5$

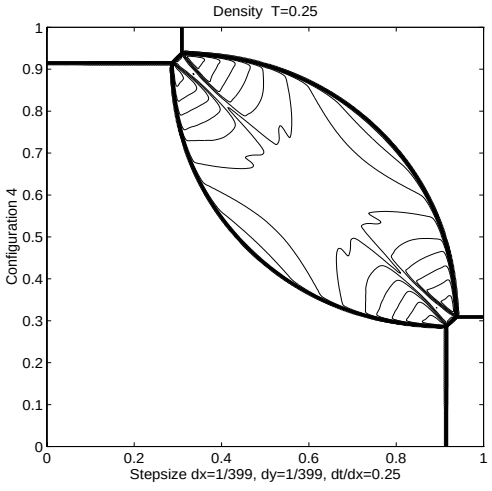

FIG. 4

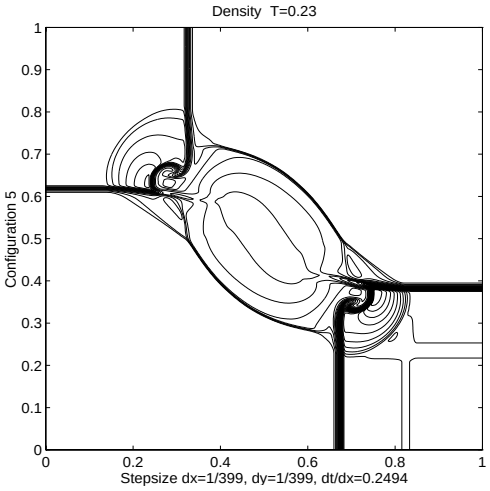

FIG. 5

CONFIGURATION 6. J^+_{32} $\overset{J^-_{21}}{\underset{J^-_{34}}{}}$ J^+_{41} : the initial data are

$p_2 = 1$	$\rho_2 = 2$	$p_1 = 1$	$\rho_1 = 1$
$u_2 = 0.75$	$v_2 = 0.5$	$u_1 = 0.75$	$v_1 = -0.5$
$p_3 = 1$	$\rho_3 = 1$	$p_4 = 1$	$\rho_4 = 3$
$u_3 = -0.75$	$v_3 = 0.5$	$u_4 = -0.75$	$v_4 = -0.5$

CONFIGURATION 7. J^-_{32} $\overset{\overrightarrow{R_{21}}}{\underset{J^-_{34}}{}}$ $\overrightarrow{R_{41}}$: the initial data are

$p_2 = 0.4$	$\rho_2 = 0.5197$	$p_1 = 1$	$\rho_1 = 1$
$u_2 = -0.6259$	$v_2 = 0.1$	$u_1 = 0.1$	$v_1 = 0.1$
$p_3 = 0.4$	$\rho_3 = 0.8$	$p_4 = 0.4$	$\rho_4 = 0.5197$
$u_3 = 0.1$	$v_3 = 0.1$	$u_4 = 0.1$	$v_4 = -0.6259$

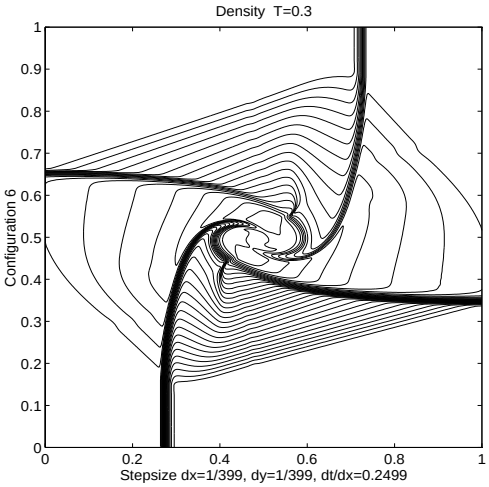

FIG. 6

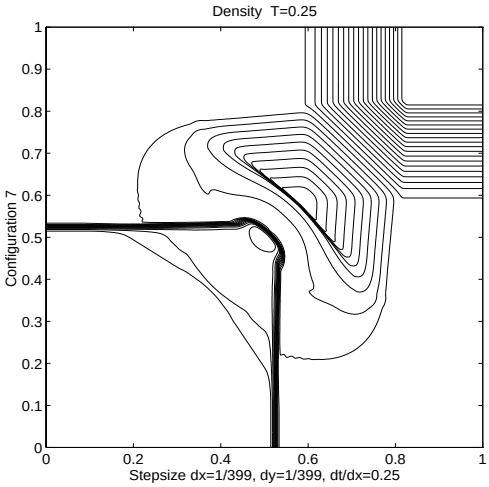

FIG. 7

CONFIGURATION 8. J^-_{32} $\overset{\overleftarrow{R_{21}}}{\underset{J^-_{34}}{}}$ $\overleftarrow{R_{41}}$: the initial data are

$p_2 = 1$	$\rho_2 = 1$	$p_1 = 0.4$	$\rho_1 = 0.5197$
$u_2 = -0.6259$	$v_2 = 0.1$	$u_1 = 0.1$	$v_1 = 0.1$
$p_3 = 1$	$\rho_3 = 0.8$	$p_4 = 1$	$\rho_4 = 1$
$u_3 = 0.1$	$v_3 = 0.1$	$u_4 = 0.1$	$v_4 = -0.6259$

CONFIGURATION 9. $\overrightarrow{R_{32}}$ $\overset{J^+_{21}}{\underset{J^+_{34}}{}}$ $\overrightarrow{R_{41}}$: the initial data are

$p_2 = 1$	$\rho_2 = 2$	$p_1 = 1$	$\rho_1 = 1$
$u_2 = 0$	$v_2 = -0.3$	$u_1 = 0$	$v_1 = 0.3$
$p_3 = 0.4$	$\rho_3 = 1.039$	$p_4 = 0.4$	$\rho_4 = 0.5197$
$u_3 = 0$	$v_3 = -0.8133$	$u_4 = 0$	$v_4 = -0.4259$

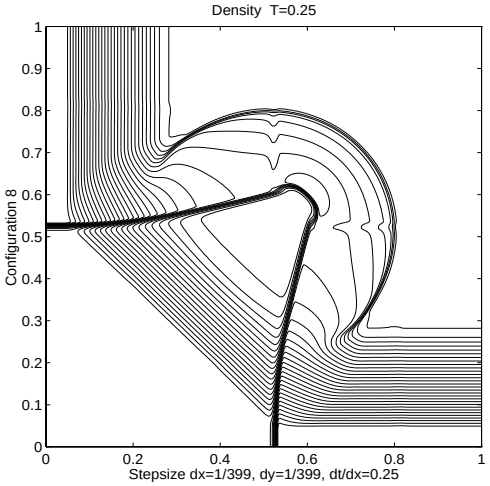

FIG. 8

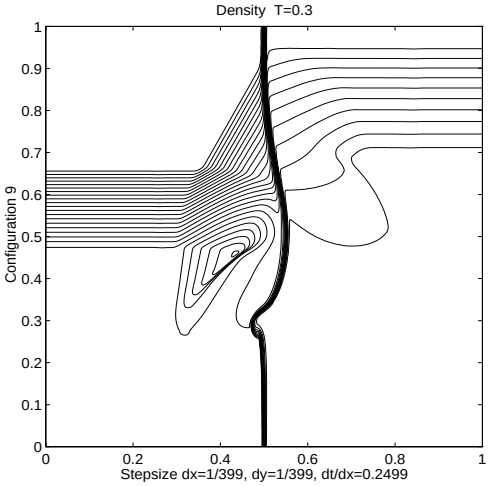

FIG. 9

CONFIGURATION 10. $\overrightarrow{R_{32}}^{J_{21}^-}\ \overrightarrow{R_{41}}^{J_{34}^+}$: the initial data are

$p_2 = 1$	$\rho_2 = 0.5$	$p_1 = 1$	$\rho_1 = 1$
$u_2 = 0$	$v_2 = 0.6076$	$u_1 = 0$	$v_1 = 0.4297$
$p_3 = 0.3333$	$\rho_3 = 0.2281$	$p_4 = 0.3333$	$\rho_4 = 0.4562$
$u_3 = 0$	$v_3 = -0.6076$	$u_4 = 0$	$v_4 = -0.4297$

CONFIGURATION 11. $J_{32}^+\ \overleftarrow{S_{21}}^{J_{34}^+}\ \overleftarrow{S_{41}}$: the initial data are

$p_2 = 0.4$	$\rho_2 = 0.5313$	$p_1 = 1$	$\rho_1 = 1$
$u_2 = 0.8276$	$v_2 = 0$	$u_1 = 0.1$	$v_1 = 0$
$p_3 = 0.4$	$\rho_3 = 0.8$	$p_4 = 0.4$	$\rho_4 = 0.5313$
$u_3 = 0.1$	$v_3 = 0$	$u_4 = 0.1$	$v_4 = 0.7276$

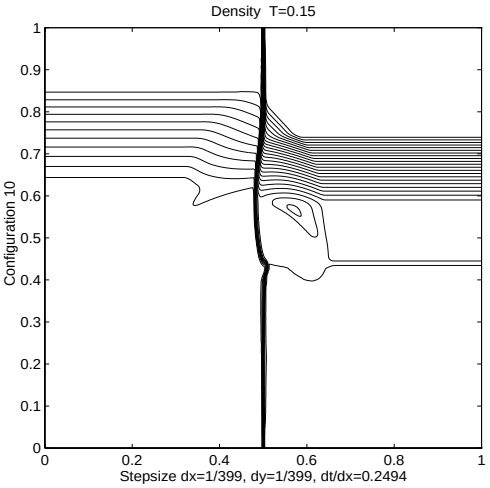

FIG. 10

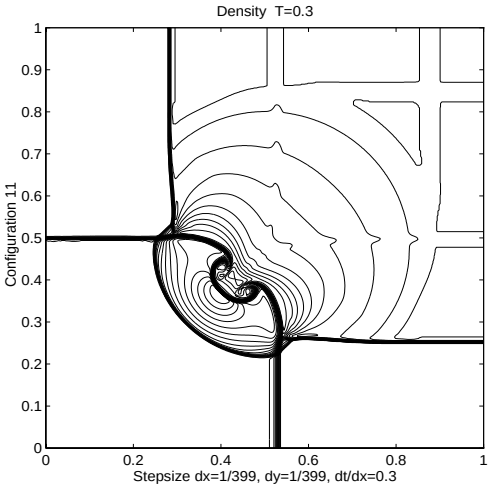

FIG. 11

CONFIGURATION 12. $J_{32}^+\ \overrightarrow{S_{21}}^{J_{34}^+}\ \overrightarrow{S_{41}}$: the initial data are

$p_2 = 1$	$\rho_2 = 1$	$p_1 = 0.4$	$\rho_1 = 0.5313$
$u_2 = 0.7276$	$v_2 = 0$	$u_1 = 0$	$v_1 = 0$
$p_3 = 1$	$\rho_3 = 0.8$	$p_4 = 1$	$\rho_4 = 1$
$u_3 = 0$	$v_3 = 0$	$u_4 = 0$	$v_4 = 0.7276$

CONFIGURATION 13. $\overleftarrow{S_{32}}^{J_{21}^-}$ $\overleftarrow{S_{41}}^{J_{34}^-}$: the initial data are

$p_2 = 1$	$\rho_2 = 2$	$p_1 = 1$	$\rho_1 = 1$
$u_2 = 0$	$v_2 = 0.3$	$u_1 = 0$	$v_1 = -0.3$
$p_3 = 0.4$	$\rho_3 = 1.0625$	$p_4 = 0.4$	$\rho_4 = 0.5313$
$u_3 = 0$	$v_3 = 0.8145$	$u_4 = 0$	$v_4 = 0.4276$

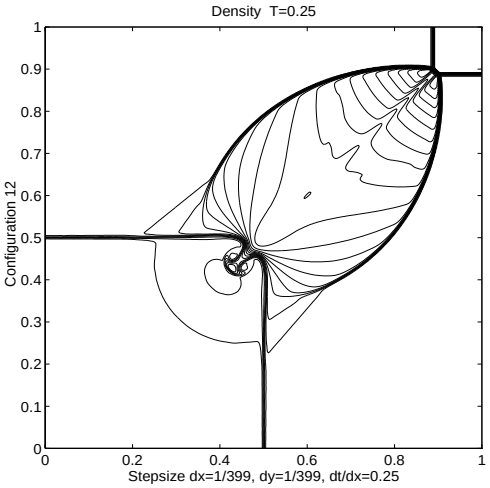

FIG. 12

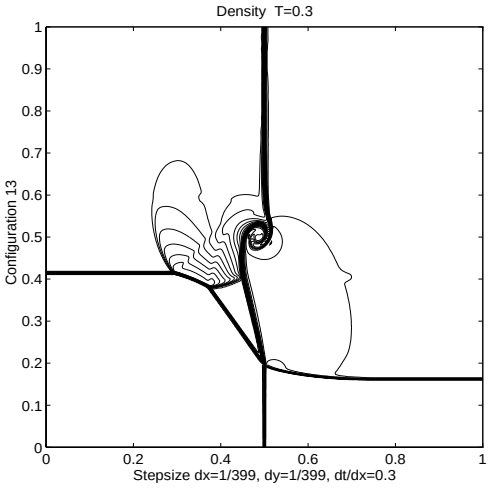

FIG. 13

CONFIGURATION 14. $\overleftarrow{S_{32}}^{J_{21}^+}$ $\overleftarrow{S_{41}}^{J_{34}^-}$: the initial data are

$p_2 = 8$	$\rho_2 = 1$	$p_1 = 8$	$\rho_1 = 2$
$u_2 = 0$	$v_2 = -1.2172$	$u_1 = 0$	$v_1 = -0.5606$
$p_3 = 2.6667$	$\rho_3 = 0.4736$	$p_4 = 2.6667$	$\rho_4 = 0.9474$
$u_3 = 0$	$v_3 = 1.2172$	$u_4 = 0$	$v_4 = 1.1606$

CONFIGURATION 15. J_{32}^- $\overrightarrow{R_{21}}$ $\overleftarrow{S_{41}}^{J_{34}^+}$: the initial data are

$p_2 = 0.4$	$\rho_2 = 0.5197$	$p_1 = 1$	$\rho_1 = 1$
$u_2 = -0.6259$	$v_2 = -0.3$	$u_1 = 0.1$	$v_1 = -0.3$
$p_3 = 0.4$	$\rho_3 = 0.8$	$p_4 = 0.4$	$\rho_4 = 0.5313$
$u_3 = 0.1$	$v_3 = -0.3$	$u_4 = 0.1$	$v_4 = 0.4276$

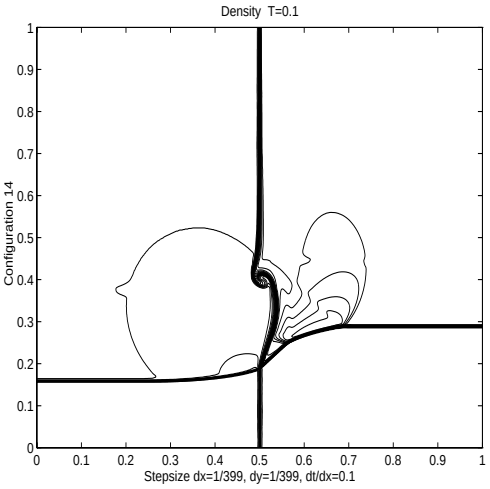

FIG. 14

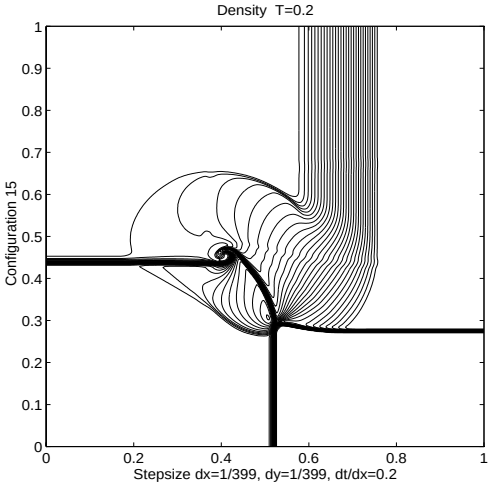

FIG. 15

CONFIGURATION 16. $\overleftarrow{R_{21}}$ J_{32}^{-} $\overrightarrow{S_{41}}$ J_{34}^{+} : the initial data are

$p_2 = 1$	$\rho_2 = 1.0222$	$p_1 = 0.4$	$\rho_1 = 0.5313$
$u_2 = -0.6179$	$v_2 = 0.1$	$u_1 = 0.1$	$v_1 = 0.1$
$p_3 = 1$	$\rho_3 = 0.8$	$p_4 = 1$	$\rho_4 = 1$
$u_3 = 0.1$	$v_3 = 0.1$	$u_4 = 0.1$	$v_4 = 0.8276$

CONFIGURATION 17. $\overleftarrow{S_{32}}$ J_{21}^{-} $\overrightarrow{R_{41}}$ J_{34}^{-} : the initial data are

$p_2 = 1$	$\rho_2 = 2$	$p_1 = 1$	$\rho_1 = 1$
$u_2 = 0$	$v_2 = -0.3$	$u_1 = 0$	$v_1 = -0.4$
$p_3 = 0.4$	$\rho_3 = 1.0625$	$p_4 = 0.4$	$\rho_4 = 0.5197$
$u_3 = 0$	$v_3 = 0.2145$	$u_4 = 0$	$v_4 = -1.1259$

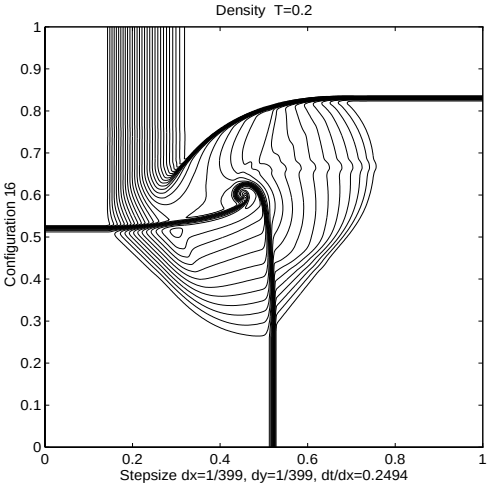

FIG. 16

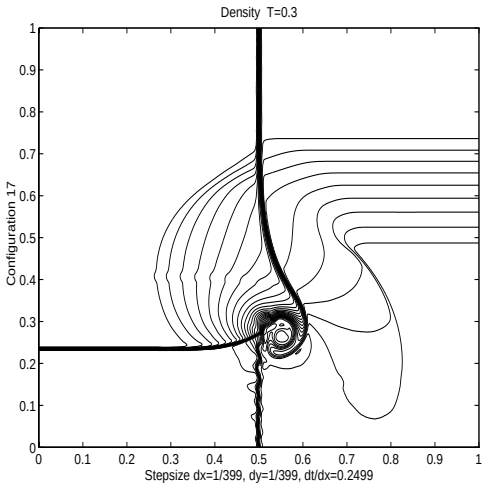

FIG. 17

CONFIGURATION 18. $\overleftarrow{S_{32}}$ J_{21}^{+} $\overrightarrow{R_{41}}$ J_{34}^{+} : the initial data are

$p_2 = 1$	$\rho_2 = 2$	$p_1 = 1$	$\rho_1 = 1$
$u_2 = 0$	$v_2 = -0.3$	$u_1 = 0$	$v_1 = 1$
$p_3 = 0.4$	$\rho_3 = 1.0625$	$p_4 = 0.4$	$\rho_4 = 0.5197$
$u_3 = 0$	$v_3 = 0.2145$	$u_4 = 0$	$v_4 = 0.2741$

CONFIGURATION 19. $\overleftarrow{S_{32}}$ J_{21}^{+} $\overrightarrow{R_{41}}$ J_{34}^{-} : the initial data are

$p_2 = 1$	$\rho_2 = 2$	$p_1 = 1$	$\rho_1 = 1$
$u_2 = 0$	$v_2 = -0.3$	$u_1 = 0$	$v_1 = 0.3$
$p_3 = 0.4$	$\rho_3 = 1.0625$	$p_4 = 0.4$	$\rho_4 = 0.5197$
$u_3 = 0$	$v_3 = 0.2145$	$u_4 = 0$	$v_4 = -0.4259$

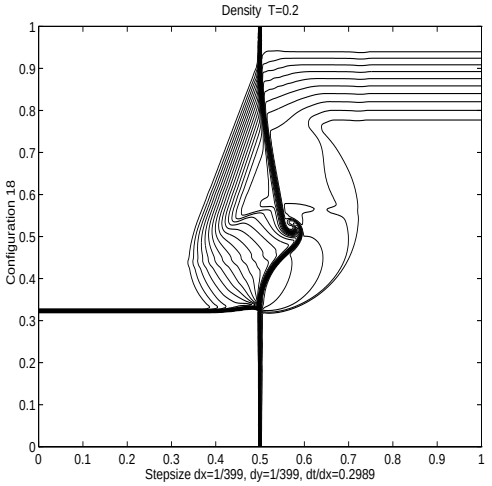

FIG. 18

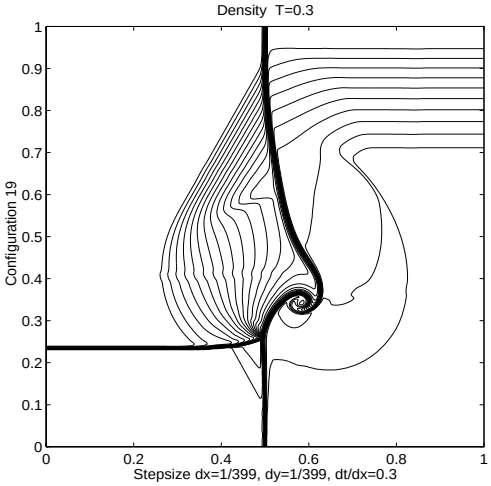

FIG. 19

In the following set of numerical experiments, we recalculate some of the configurations by using different parameters $\alpha = 1$, $\beta = 0.01$, and Superbee limiter for $\phi_k^0(\theta^k)$ for the linear fields, i.e., $k = 2, 3$, and vanLeer's limiter for $\phi_k^0(\theta^k)$ for the others, i.e., $k = 1, 4$. The initial data were chosen the same as before.

CONFIGURATION 5. J_{32}^- $\begin{matrix} J_{21}^- \\ J_{34}^- \end{matrix}$ J_{41}^- : The density contours of the solutions under different resolutions are shown in Figures 20 and 21.

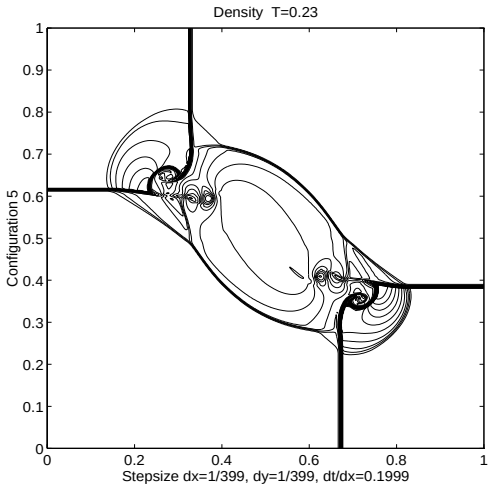

FIG. 20

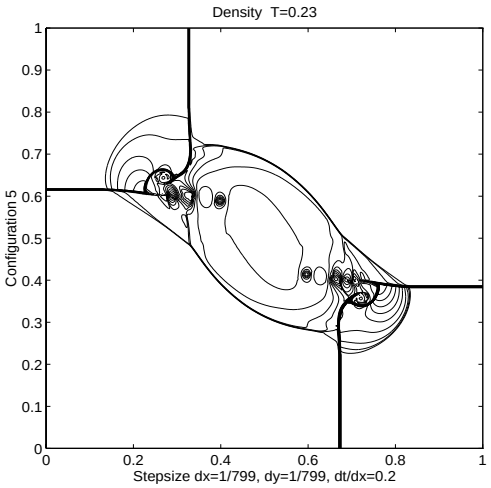

FIG. 21

CONFIGURATION 6. J_{32}^+ $\begin{matrix} J_{21}^- \\ J_{34}^- \end{matrix}$ J_{41}^+ : The density contours of the solutions are shown in Figure 22.

CONFIGURATION 11. J_{32}^+ $\begin{matrix} \overleftarrow{S_{21}} \\ J_{34}^+ \end{matrix}$ $\overleftarrow{S_{41}}$: The density contours of the solutions are shown in Figure 23.

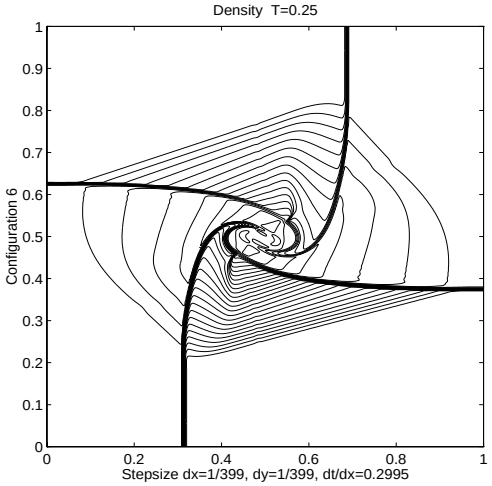

FIG. 22

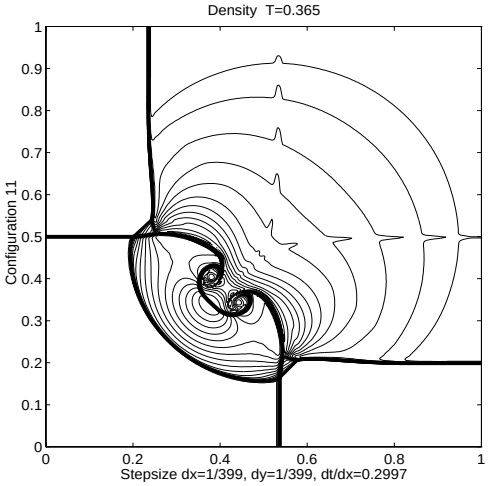

FIG. 23

5. Discussion. With fixed parameters in the first set of experiments our numerical results are strikingly consistent with calculations by Schulz-Rinne, Collins, and Glaz [9] for the same configurations with the same initial data.

In the second set of experiments the slip lines in Figures 20 and 21 are much thinner than ones in Figure 5; more vortices are seen in Figure 21 than in Figure 20; as the calculations are refined the number of vortices might well tend to infinity.

In Figure 17 we observe an incipient instability of the slip line; no such instability occurs in Figure 19. This difference may be due to the sign of the initial slips.

The computational results demonstrate that two-dimensional gas flow with Riemann initial data are very complicated. The wave patterns include mach reflection, rolling up of slip lines, possible incipient instability of slip lines, and much more. The complicated wave patterns indicate that a Glimm type of estimate [4] in two space dimensions seems very unlikely; also, any scheme based on genuinely multidimensional Riemann solvers would be very complicated.

REFERENCES

[1] P. COLELLA AND H. M. GLAZ, *Efficient solution algorithms for the Riemann problem for real gases*, J. Comput. Phys., 59 (1985), pp. 264–289.

[2] P. COLELLA AND P. WOODWARD, *The piecewise parabolic method (PPM) for gas-dynamical simulations*, J. Comput. Phys., 54 (1984), pp. 174–201.

[3] R. COURANT AND K. O. FRIEDRICHS, *Supersonic Flow and Shock Waves*, Springer-Verlag, New York, 1948.

[4] J. GLIMM, *Solutions in the large for nonlinear hyperbolic systems of equations*, Comm. Pure Appl. Math., 18 (1965), pp. 697–715.

[5] A. HARTEN, *On a class of high resolution total-variation-stable finite-difference schemes*, SIAM J. Numer. Anal., 21 (1984), pp. 1–23.

[6] T.-P. LIU, *Admissible solutions of hyperbolic conservation laws*, Mem. Amer. Math. Soc., No. 240, 30 (1981).

[7] X.-D. LIU AND P. D. LAX, *Positive Schemes for Solving Multi-dimensional Hyperbolic Systems of Conservation Laws*, J. Comp. Fluid Dynam., 5 (1996), pp. 133–156.

[8] C. W. SCHULZ-RINNE, *Classification of the Riemann problem for two-dimensional gas dynamics*, SIAM J. Math. Anal., 24 (1993), pp. 76–88.

[9] C. W. SCHULZ-RINNE, J. P. COLLINS, AND H. M. GLAZ, *Numerical solution of the Riemann problem for two-dimensional gas dynamics*, SIAM J. Sci. Comput., 14 (1993), pp. 1394–1414.

[10] C.-W. Shu, *Total-variation-diminishing time discretizations*, SIAM J. Sci. Statist. Comput., 9 (1988), pp. 1073–1084.
[11] C.-W. Shu and S. Osher, *Efficient implementation of essentially non-oscillatory shock-capturing schemes*, II, J. Comput. Phys., 83 (1989), pp. 32–78.
[12] G. Strang, *On the construction and comparison of difference schemes*, SIAM J. Numer. Anal., 5 (1968), pp. 506–517.
[13] T. Zhang and Y. Zheng, *Conjecture on the structure of solutions of the Riemann problem for two-dimensional gas dynamics systems*, SIAM J. Math. Anal., 21 (1990), pp. 593–630.
[14] T. Zhang, G.-Q. Chen, and S. Yang, *On the* 2*-D Riemann problem for the compressible Euler equations,* I. *Interaction of shocks and rarefaction waves*, Discrete Continuous Dynam. Systems, 1 (1955), pp. 555–584.